Multiwavelength distributed Bragg reflector laser array fabricated using near field holographic printing with an electron-beam generated phase grating mask

D. M. Tennant, T. L. Koch, J-M. Verdiell, K. Feder, R. P. Gnall, U. Koren, M. G. Young, B. I. Miller, M. A. Newkirk, and B. Tell
AT&T Bell Laboratories, Holmdel, New Jersey 07733

(Received 21 June 1993; accepted 30 July 1993)

We describe near optimum near field holography grating masks patterned by e-beam lithography and a distributed Bragg reflector (DBR) multiwavelength laser array fabricated using near field printing with this mask. Grating pitches in the array ranged from 242.861 to 243.750 nm in 0.127 nm steps. Data on the pitch precision and pitch adjustment is presented. Use of a conventional UV source rather than laser illumination both greatly simplified the printing process and eliminated coherent artifacts from the printed gratings. Chemically etched InP test gratings are shown to be extremely "clean" in appearance and low in edge roughness. DBR laser arrays designed with 100 GHz frequency separation were processed using the mask described. The measured frequency separation was 99 GHz which could be further adjusted with a tuning section of the four-section laser design. Characterization of a similar grating mask containing 16 wavelengths with similar pitch increments is also described.

I. INTRODUCTION

Near field holographic (NFH) printing of gratings has been demonstrated to be a promising alternative to conventional holographic methods.[1-3] When patterned using a flexible patterning technique such as electron or ion beam lithography,[2,3] NFH masks can incorporate high resolution gratings, phase shifted gratings, etc., into a single lithography step. In addition, the process of producing fine pitch gratings with NFH masks is greatly simplified by using a slightly modified UV contact aligner. In this paper we present data on a near optimum fused silica mask with e-beam written pure phase gratings and on distributed Bragg reflector (DBR) lasers fabricated using near field holographic exposures with this mask. The mask contains 960 grating sites comprising 120 repeats of 8 different grating pitches. Grating pitch designs ranged from 242.861 to 243.750 nm in 0.127 nm steps. Resultant grating pitches and pitch changes were measured using first order diffraction angles and angle changes, respectively. Nearly balanced power into the zero and first order orthogonally polarized diffracted beams was achieved by optimizing the etch depth, grating profile, and duty cycle.[2,4] The mask was carefully characterized, with special attention paid to artifacts potentially introduced by electron-beam lithography, and then used to print gratings on both device and nondevice wafers. Use of a conventional UV source rather than laser illumination is described that both greatly simplified the printing process and eliminated coherent artifacts in the printed gratings. Fabrication and performance of a device lot of DBR laser arrays designed with 100 GHz frequency separation is reported.

II. GRATING MASK FABRICATION AND CHARACTERIZATION

The extremely fine changes in period required for wavelength division multiplexing (WDM) for light wave communications cannot be achieved using straightforward means of encoded patterns of various periods (Λ). This approach can suffer from discretization minima in the address structure. In our approach we make use of a fine gain adjustment made to the e-beam system while using a coded 250 nm period grating pattern. While this adjustment is normally used to correct the system metrology during the writing session, it can also be used to intentionally stretch or shrink each axis. The DAC setting in our system permits a 12-bit adjustment over a 6.4% range in the gain, thus allowing 0.0039 nm changes in the grating period for this pattern. This number varies linearly, of course, with the period of the coded pattern. Since the overall gains in x and y are adjusted (independently), any phase shifting section of the grating is expanded or shrunk by the same relative amount. Therefore a $\Lambda/2$ ($\lambda/4$) phase shift initially coded into the grating pattern remains the same fraction of the period even after adjustment.

The square wave pure phase gratings are fabricated essentially as previously reported.[2] The gratings are patterned using e-beam lithography in a trilayer resist process. More reliable performance and smoother gratings were obtained using a PMMA imaging layer, however, and was therefore used for the results reported here. The developed e-beam written pattern is transferred into the middle and lower layer of the trilayer resist and then into the fused silica mask using reactive ion etching as previously reported.

The diffraction efficiency of the resultant fused silica grating is dependent on the etched depth, duty cycle, and tooth shape.[2,4] For all the gratings reported here, a standard groove depth of 22–25 nm is maintained. The depths of etch monitor features (30 μm squares) are measured using a scanning stylus profilometer to verify the groove depth. We determined by scanning electron microscopy (SEM) analysis on cleaved gratings that the monitor depth

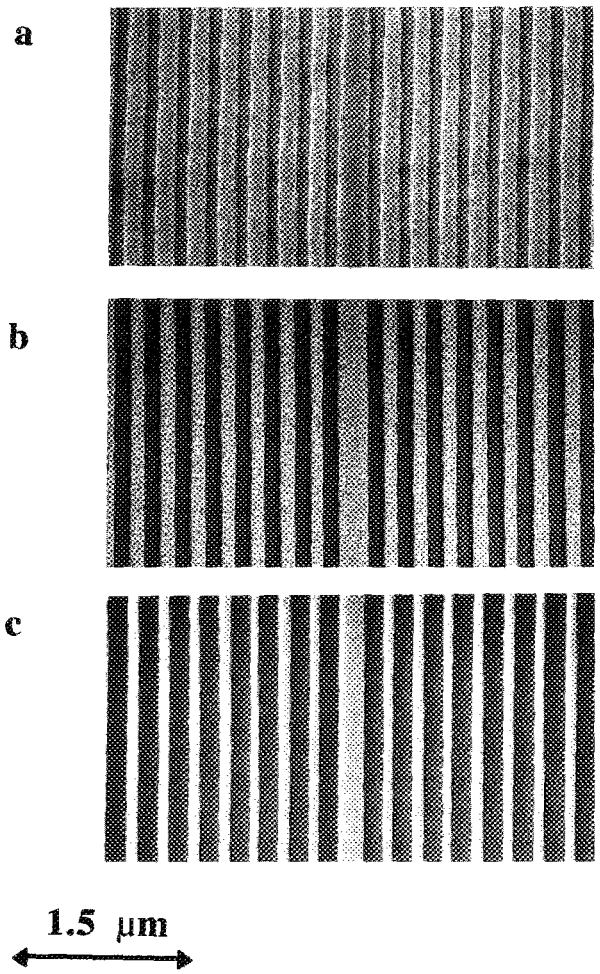

FIG. 1. Top view SEMs of a NFH mask under fabrication. (a) Top PMMA layer after development; (b) after the RIE of the middle and lower layers of the trilevel resist; (c) the completed grating etched in fused silica.

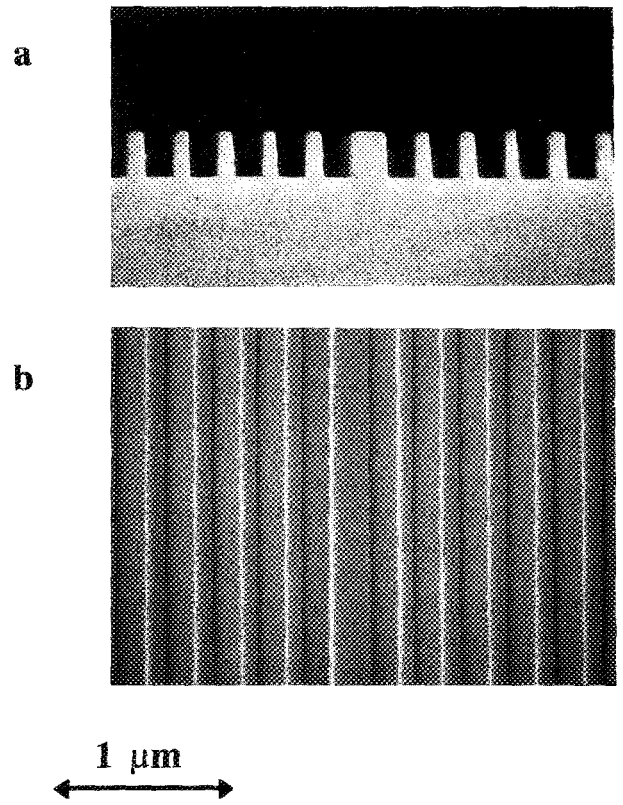

FIG. 2. Top and cross-sectional view SEMs of the completed phase grating in fused silica showing the near ideal groove profile and smooth edges produced using this process.

is representative of the groove depth. There appears to be no significant reactive ion etching (RIE) lag. The duty cycle is the principal variant in determining the diffraction efficiency. Our previous study empirically determined that the best balance between the diffracted (first order) and transmitted (zero order) beams are not obtained for 50% duty cycle. Rather a tooth width (l) and groove width (s) in a ratio (l/s) of 0.5 is optimum. To approach a 33% duty cycle in the fused silica grating, the initial lithography is biased to obtain narrower developed openings (40%) and wider remaining resist (60%). This compensates for a general widening of the grooves as the various RIE steps are completed. Figure 1 shows SEM micrographs of this patterned (a) etched trilevel (b) and completed grating (c). A SEM of a representative cross sectional and plan view of the grating is shown in Fig. 2. We observe that while the profiles are not perfect, they are nearly square in profile and more than adequate to produce high contrast interference patterns. The small differences from ideal, however, may account for some of the departure from the theoretical diffraction efficiencies.[2,4]

The performance of the grating masks is best predicted by measuring the period, period increment (in the multiwavelength masks), and the ratio of the zero to first order diffracted powers. The period is determined by precisely measuring the first-order diffraction angle when illuminated with an argon ion laser ($\lambda = 363.8$ nm). The accuracy of this absolute angle measurement is limited by our angular resolution of 4 min of arc (corresponding to about 0.24 nm). All of our gratings have been consistently within this uncertainty of their design period. For the period increment measurements, a stepper motor controlled rotation stage allowed more precise measurements of the pitch changes. The minimum angle increment of the stepper motor is 0.01° that corresponds to a grating pitch change of 0.0189 nm. An eight-wave fused silica NFH mask was fashioned in a chromium coated photomask blank in which chemically etched windows in the chromium layer were opened using conventional contact photolithography. E-beam written gratings were patterned in the clear window device sights. The mask layout comprised 48 rows (on 508 μm centers) and 20 columns (on 1.27 mm centers) of gratings, each about 200 μm $\times$ 20 μm in area. The grating period was constant within each row and was varied through eight periods by increments of 0.127 nm down each column, repeating after each eight increments. The minimum design grating period was 242.861 nm and the maximum was 243.750 nm. The measured value of Λ for the maximum period was 243.87 nm, within our experi-

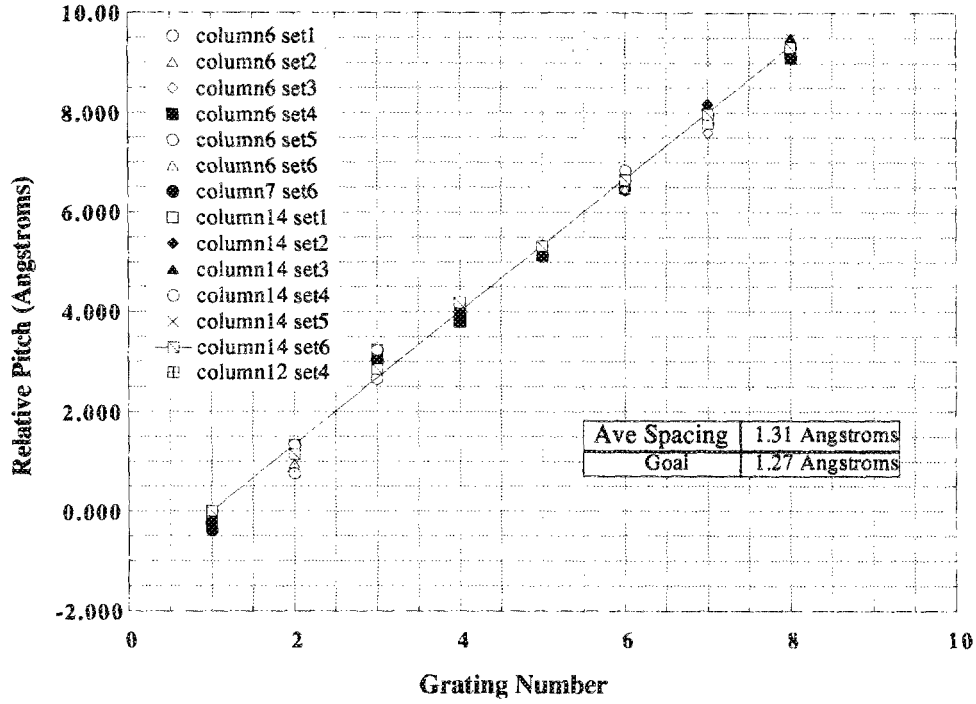

FIG. 3. Wavelength distribution of the 8-wavelength fused silica phase mask.

mental uncertainty for the absolute period setup. The wavelength difference from the fundamental period for the other seven grating types is about a factor of twelve more precise.

The measured results are plotted in Fig. 3. For each type, nine different gratings were measured which sample widely separated portions of the mask. This is a worst case representation of the uniformity since the first written gratings are separated by as much as 12 h from the last written. The average change in period, $\Delta\Lambda$, given by the slope of a

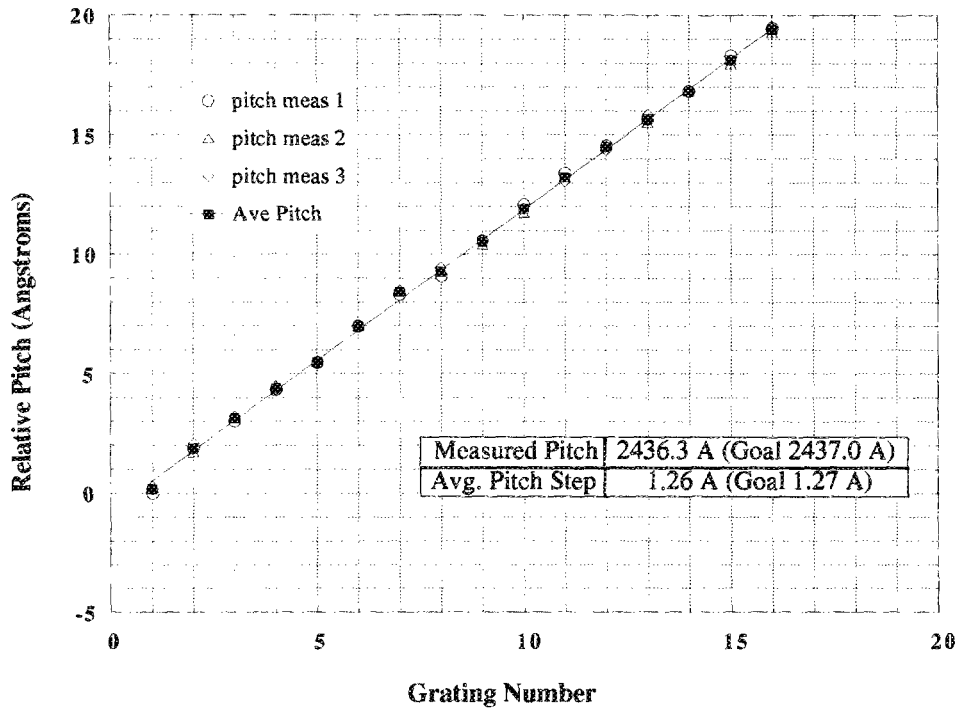

FIG. 4. Wavelength distribution of the 16-wavelength fused silica phase mask.

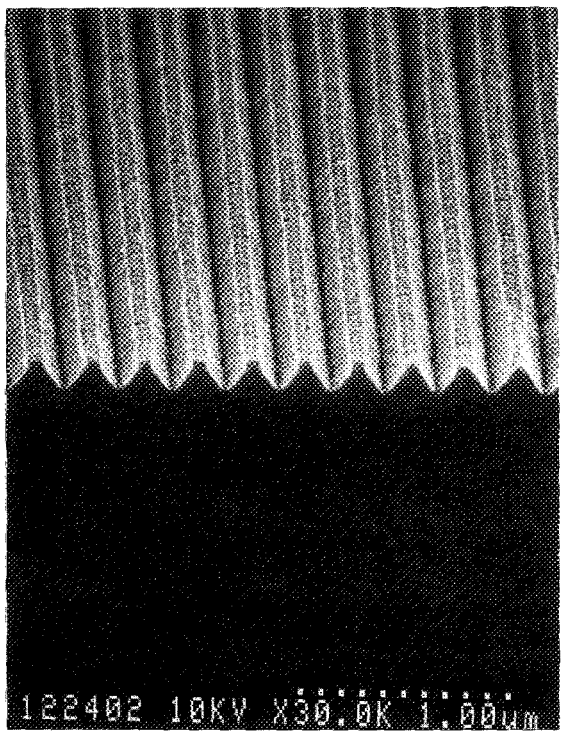

FIG. 5. SEM of the wet chemically etched gratings in InP produced using NFH with the 8-wavelength mask described in the text.

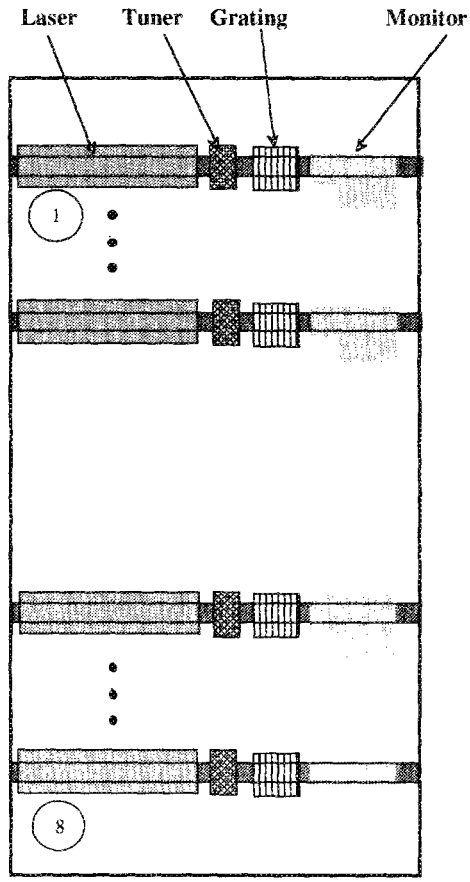

FIG. 6. Schematic of the four section DBR laser array fabricated using the 8-wavelength NFH mask.

linear fit to the data, is 0.131 nm, higher than the design goals by about one least significant bit (LSB). This mask was next used to produce the DBR laser arrays described in the following section.

A second mask design comprising 16 different grating types with similar design increments proved to be of even higher quality. The layout for this laser grouped the different gratings more closely (250 μm on center) while spacing consecutive groups more sparsely to allow for other system components. A total of 1408 gratings were written over the mask. Figure 4 summarizes the measured values of Λ and $\Delta\Lambda$ for three widely spaced gratings of each type. The absolute period is 243.63 nm, well within the measurement error of the design period of 243.7 nm, the average pitch change is 0.126 nm (the goal was 0.127 nm), and the scatter appears to be half that of the previous mask. The beam power ratio for all the gratings on both this and the previous masks fell between 1.1 and 2.05. Most of this variation is due to intentional changes in the dose of the e-beam write which results in small duty cycle variations. This range in power ratios results in a range of intensity variations (I_{max}/I_{min}) in the interference patterns of from 1760 to 32. This is more than adequate to produce good contrast in the printing process.

We have also constructed phase shifted gratings for DFB laser applications although we have not yet fabricated lasers from these masks. Our two designs include a single $\lambda/4(\Lambda/2)$ shift centered on the grating as well as a second design that includes five $\lambda/20$ ($\Lambda/10$) phase shifts distributed symmetrically about the grating. The $\Lambda/2$ shifts are present in the examples shown in Figs. 1 and 2. While we do not expect these abrupt shifts to replicate crisply, we do expect the relative phase differences between adjacent grating sections to be preserved.[2]

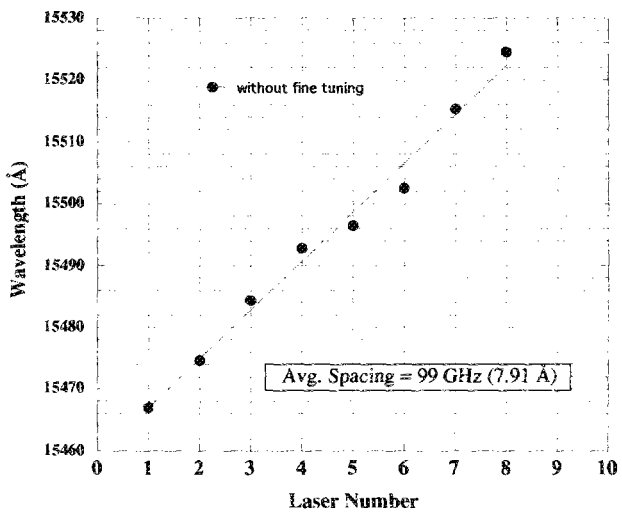

FIG. 7. Output of the 8-wavelength DBR laser array with no tuning.

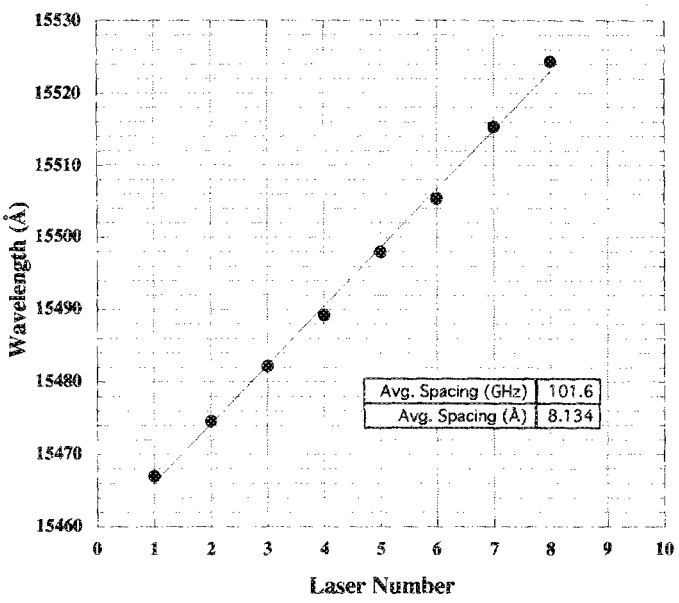

FIG. 8. Output of the 8-wavelength DBR laser array with less than 2 mA of tuning.

III. DBR LASER FABRICATION AND PERFORMANCE

Since the near field use of these gratings described requires only local spatial coherence and limited temporal coherence from the source, a conventional short arc mercury lamp can be used. We calculate that for a commercially available 100 W lamp with a 0.25 mm arc using an $f=50$ mm condenser optic and an interference filter centered at 365 nm, good fringe visibility requires a gap between the phase mask and wafer of only 12 μm or less.[5] We have therefore assembled a modified contact mask aligner to print the gratings for the DBR laser arrays. The aligner is similar to a standard system with the short arc source, filter, a polarizer, and a modified UV mirror angle. The mirror angle is adjusted so that the illumination is incident at the Bragg angle on the mask. The polarizing filter is needed since the diffraction efficiency of the grating is strongly polarization dependent.

A sample exposure was made in a 50 nm thick layer of AZ1400-3 photoresist on InP (the exposure time was 60 s). The resist was developed, postbaked at 90 °C for 30 min, then transferred into the semiconductor by wet chemical etching. The resulting etched InP gratings are extremely "clean" in appearance and low in edge roughness (Fig. 5).

We applied this NFH technique to fabrication of an array of four-section DBR lasers.[5,6] Figure 6 shows the design of the laser which combines a 840 μm long gain section, a 120 μm phase section, a 180 μm grating section, and a 100 μm integrated monitor section. The design frequency spacing is 100 GHz (0.813 nm in air) between lasers. The laser material and fabrication process is reported elsewhere.[6] The completed lasers exhibited thresholds of less than 30 mA. The lasers were biased at about 50 mA and exhibited the wavelength distribution plotted in Fig. 7 with no tuning. The average frequency spacing was 99 GHz within 1 GHz of the design goal. The scatter is in part due to random mode placement within the more evenly spaced Bragg bands. Fine tuning using current injection in the phase and grating sections can further improve the wavelength distribution. Figure 8 shows the nearly ideal characteristics attained with less than 2 mA applied to any section.

IV. CONCLUSIONS

We have demonstrated that NFH implemented with an e-beam written grating mask exhibits comparable precision to conventional holographic exposures in both absolute pitch and pitch increment for WDM applications.

The grating masks readily provide adequate image contrast and are compatible with contact printing in a modified aligner. This allows that level to level alignment can be performed and that the process can set up in a clean room environment. The e-beam patterning on the mask is a flexible patterning method which permits a variety of grating types and other (larger) features to be combined in a single printing step.

The gratings printed from the phase masks are comparable or better to those printed in the conventional holographic manner. Coherent artifacts usually evident in the laser holography process are greatly reduced with the incoherent source.

The 8-wavelength laser array with 100 GHz channel spacing fabricated with the NFH process exhibited low thresholds and excellent wavelength control. The high quality lasers produced, combined with good pitch control reported provides strong evidence that e-beam generated phase masks can replace current holographic techniques for a wide class of light wave component applications.

[1]M. Okai, S. Tsuji, N. Chinone, and T. Harada, Appl. Phys. Lett. **55**, 415 (1989).
[2]D. M. Tennant, T. L. Koch, P. P. Mulgrew, R. P. Gnall, F. Ostermayer, and J-M. Verdiell, J. Vac. Sci. Technol. B **10**, 2530 (1992).
[3]G. Pakulski, R. Moore, C. Maritan, F. Shephard, M. Fallahi, I. Templeton, and G. Champion, Appl. Phys. Lett. **62**, 222 (1993).
[4]M. G. Moharam and T. K. Gaylord, J. Opt. Soc. Am. **72**, 1385 (1982).
[5]J-M. Verdiell, T. L. Koch, D. M. Tennant, K. Feder, R. P. Gnall, M. G. Young, B. I. Miller, U. Koren, M. A. Newkirk, and B. Tell, Proceedings of the European Conference Integrated Optics, Neuchatrel, Switzerland, 1993 (unpublished), p 4.8.
[6]T. L. Koch, U. Koren, and B. I. Miller, Appl. Phys. Lett. **53**, 1030 (1988).